JOURNAL OF GEOPHYSICAL RESEARCH, VOL. 112, B12201, doi:10.1029/2006JB004582, 2007

Fractal characterization of fracture networks: An improved box-counting technique

Ankur Roy,[1] Edmund Perfect,[1] William M. Dunne,[1] and Larry D. McKay[1]

Received 19 June 2006; revised 6 June 2007; accepted 5 September 2007; published 5 December 2007.

[1] Box counting is widely used for characterizing fracture networks as fractals and estimating their fractal dimensions (D). If this analysis yields a power law distribution given by $N \propto r^{-D}$, where N is the number of boxes containing one or more fractures and r is the box size, then the network is considered to be fractal. However, researchers are divided in their opinion about which is the best box-counting algorithm to use, or whether fracture networks are indeed fractals. A synthetic fractal fracture network with a known D value was used to develop a new algorithm for the box-counting method that returns improved estimates of D. The method is based on identifying the lower limit of fractal behavior (r_{cutoff}) using the condition $ds/dr \rightarrow 0$, where s is the standard deviation from a linear regression equation fitted to $\log(N)$ versus $\log(r)$ with data for $r < r_{cutoff}$ sequentially excluded. A set of 7 nested fracture maps from the Hornelen Basin, Norway was used to test the improved method and demonstrate its accuracy for natural patterns. We also reanalyzed a suite of 17 fracture trace maps that had previously been evaluated for their fractal nature. The improved estimates of D for these maps ranged from 1.56 ± 0.02 to 1.79 ± 0.02, and were much greater than the original estimates. These higher D values imply a greater degree of fracture connectivity and thus increased propensity for fracture flow and the transport of miscible or immiscible chemicals.

Citation: Roy, A., E. Perfect, W. M. Dunne, and L. D. McKay (2007), Fractal characterization of fracture networks: An improved box-counting technique, *J. Geophys. Res.*, *112*, B12201, doi:10.1029/2006JB004582.

1. Introduction

[2] Fracture systems have been a focus of research for decades owing to their importance in contexts such as hydrocarbon accumulation, contaminant transport, engineering geology and seismogenic faults. Fractures exist over a wide range of scales, from microns (in thin sections) to thousands of kilometers (as with plate-bounding faults). They typically develop more complex patterns in a region as fracturing events are superimposed through time. This combination of characteristics potentially makes them interesting targets for fractal analyses.

[3] Fractals are entities that display self-similarity in their geometry such that any portion of the system is a replica of the whole as seen at a larger scale. This scaling is quantified by the fractal dimension. In simplistic terms, the fractal dimension describes the manner in which a fractal entity fills up the available Euclidean space. More precisely, *Mandelbrot* [1983] defines a fractal as a set for which the Hausdorff-Besicovitch dimension (D) strictly exceeds the topological dimension. Every set with a noninteger D value is a fractal, but it is not necessary that all fractal dimensions be nonintegers. Since we are dealing with linear fractures in two dimensions, noninteger fractal dimensions are expected within the range $1 < D < 2$.

[4] Many researchers have reported fractal dimensions for natural fracture patterns. Details on most of these works, along with critiques of the methods used, can be found in the review paper by *Bonnet et al.* [2001]. A few studies have related fractal dimensions of fracture networks to physical properties such as the percolation threshold [*Zhang and Sanderson*, 1994] and dynamic processes such as flow and transport [*Doughty and Karasaki*, 2002]. Small differences in D can have a profound impact on these properties and processes; thus it is vital that methods of estimating D are both accurate and precise.

[5] The most popular method for determining the fractal dimension of a fracture pattern is the box-counting algorithm. In its most basic form, this method involves superimposing smaller and smaller square grids of normalized length, r (where r is box length divided the characteristic length of the mapped area) upon the mapped network. The number of occupied boxes containing one or more fractures, $N_{occupied}$, is given by

$$N_{occupied} = r^{-D_b} \quad (1)$$

where D_b is the box-counting fractal dimension. Equation (1) holds for $r_{min} < r < r_{max}$, where r_{max} and r_{min} are the upper and lower limits of fractal scaling, respectively. As r is systematically reduced in size within this range, equation (1) yields an array of points in log-log

[1]Department of Earth and Planetary Sciences, University of Tennessee, Knoxville, Tennessee, USA.

0148-0227/07/2006JB004582$09.00

space that can be fitted with a straight line whose negative slope (D_b) is equal to the D value for the fracture pattern.

[6] Numerous variations of this technique exist in the literature. In order to accommodate a boundary condition stated by *Hausdorff* [1919] and incorporated into the derivation of equation (1), it is required in the box-counting algorithm to find the minimum number of occupied cells for each cell size. Numerically, this may be achieved in two ways [*Pruess*, 1995]. One approach involves rotating the grid relative to the data until the minimum number of occupied cells is attained [*Samuel*, 1988]. This is called the box rotate method [*Barton*, 1995]. Alternatively, if the scale factor, $\beta > 1$, governing the progressive reduction in r ($r = \beta^{-j}$, where j is an integer iteration level) is minimized, the number of occupied cells for a given size can also be minimized [*Pruess*, 1995]. This approach is called the box flex method [*Barton*, 1995]. *Barton* [1995] concluded that the box flex method provides more accurate results than the box rotate method.

[7] Two other versions of the box-counting algorithm are documented by *La Pointe* [1988]. One involves counting the number of fractures within each cell of the box-counting grid. This information is then used to assign a third dimension to the data set, with the fractal dimension being determined by the extent to which this surface fills the available volume. A problem with this method is that the resulting D_b value ends up being greater than two. The other version counts the number of blocks bounded by fractures within each cell. Obviously, this algorithm cannot be employed for very sparse fracture networks (with relatively low fractal dimensions), since there may be insufficient intersections to define any blocks.

[8] In spite of the large number of investigations, researchers are still divided in their opinions as to whether fracture networks can be characterized as fractals [e.g., *Gillespie et al.*, 1993; *Walsh and Watterson*, 1993]. Also, since different workers have reported different values of the fractal dimension for the same map, a technique for evaluating the fractal dimension of fracture patterns that has wide acceptance remains to be developed.

[9] Our research addresses these questions by developing an improved version of the box-counting method. The method is validated for a synthetic fracture network with a known D value and then applied to a natural fracture pattern mapped at 7 different resolutions [*Odling*, 1997] and 17 fracture trace maps from a variety of tectonic settings, lithologies and scales [*Barton*, 1995]. We show the method yields improved estimates of D, and the results are briefly considered in the context of network connectivity.

2. Method Development

2.1. Synthetic Fractal Fracture Patterns

[10] Synthetic fractal fracture patterns were constructed using a generalized version of *Sammis et al.*'s [1986] self-similar cataclasis model. *Doughty and Karasaki* [2002] employed essentially the same approach for simulating flow through hierarchically fractured rocks. Fracture networks were represented as deterministic Sierpinski lattices composed of self-similar line segments in two dimensions. The lattices were generated using three parameters: the scale factor, b, the iteration level, i, and the initial number of unfractured blocks, n. The initiator ($i = 0$) consists of a unit square with b orthogonal fractures dividing the area into b^2 blocks of length $1/b$ (Figure 1a). In the next step ($i = 1$), n blocks are left unfractured, while $b^2 - n$ are fractured by copying scaled down versions of the initiator into the remaining blocks, thus creating the generator (Figure 1b). The generator is then applied onto itself in successive iterations creating a sequence of hierarchically fractured patterns (Figures 1a–1f). The spatial locations of the fractured and unfractured blocks can be selected deterministically (as was done here), or randomized at each iteration level.

[11] The number-length distribution of the fractures in this fractal model is given by

$$N_f = 2(b-1)\left(b^2-n\right)^i = 2(b-1)l^{-D} \tag{2}$$

where N_f is the number of fractures of length $l = 1/b^i$ and $D = \log(b^2 - n)/\log b$. Had we started with an initial length of λ instead of unity, the lengths in equation (2) would scale as λ/b^i instead of $1/b^i$. The term $2(b - 1)$ in equation (2) describes the number of elements in the initiator. Since the embedding Euclidean dimension is two and the initial subdivision is at 90°, fractures may form in only two directions. In each direction, the fractures divide the entire length of the embedding surface into b parts, and hence the number of fractures formed in each direction is $b - 1$. The term $(b^2 - n)^i$ in equation (2) determines the number of blocks that are fractured at each scale, thereby giving the pattern its fractal character. Equation (2) holds for any set of b and n values. It even works if the fractures are randomly oriented and their centers distributed at random.

[12] For our particular model, $b = 2$, $n = 1$, $D = \log 3/\log 2 = 1.585$, and $i = 1$–6 (Figure 1 shows the initiator and the resulting fracture patterns for iterations 1 through 5). Since D is independent of i, all of the patterns have the same fractal dimension. Using equation (2) it can be shown that the negative slope of the fracture number versus length plot on a log-log scale yields the exact theoretical fractal dimension. In the limit, $i \rightarrow \infty$, the negative slope of the cumulative fracture number versus length plot also yields the theoretical fractal dimension [*Roy*, 2006].

2.2. Analytical Box Counting

[13] The box-counting technique for determining the fractal dimension involves overlaying the pattern under investigation with a sequence of grids, each with a different cell size, r, and counting the number of occupied cells, N. This procedure can be performed both analytically and numerically. In this section, an analytical expression is developed for estimating D_b that allows for a box-counting scale factor, β, that is different from the scale factor of the underlying fractal lattice, b.

[14] We begin by constructing a synthetic fracture pattern to a given i level, $i$max, with parameters b and n. We then overlay smaller and smaller square grids of length r such that $r = \beta^{-j}$, where j is the box-counting iteration level. If $\beta = b$, then $j = i$ and $j$max = $i$max, where $j$max is the maximum number of box-counting iterations. The minimum grid size is then given by $r_{\min} = l_{\min} = 1/b^{i\max} = 1/\beta^{j\max}$, where $l_{\min}$ is the smallest fracture length in a

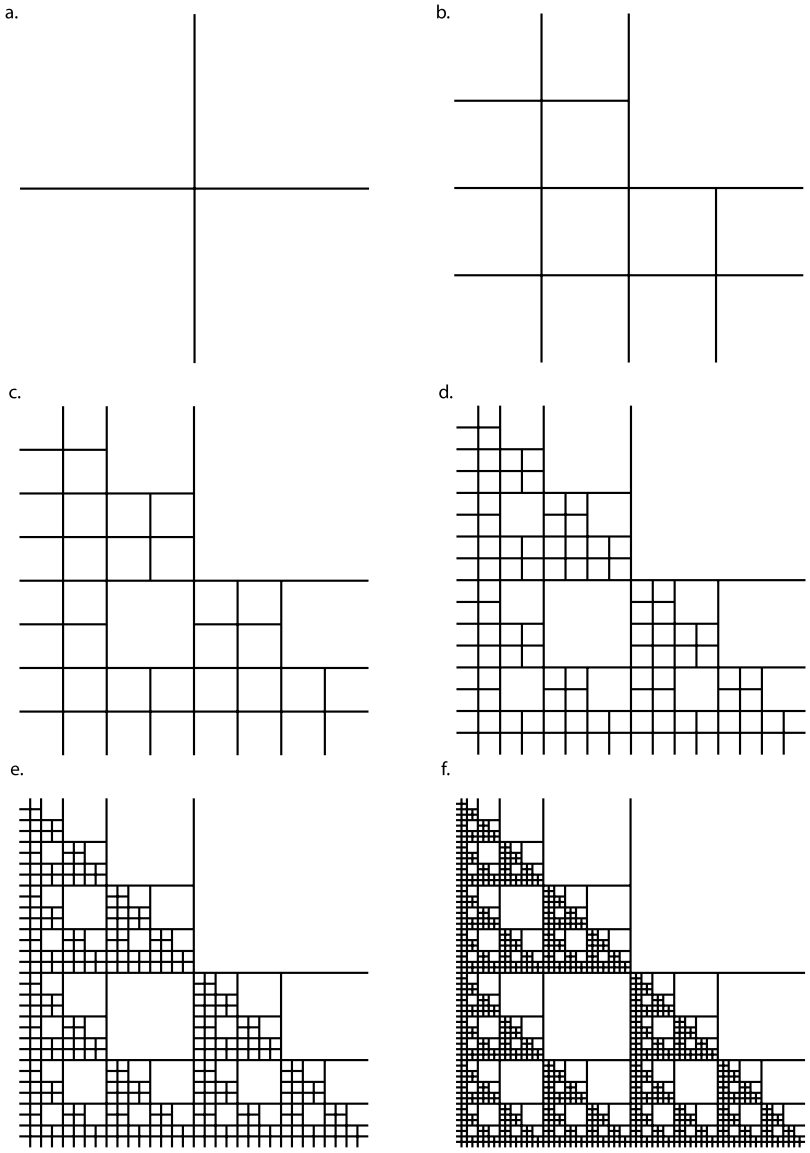

Figure 1. Construction of a deterministic Sierpinski lattice with $b = 2$ and $n = 1$, (a) basic template $i = 0$ with two fractures of length 1, (b) $i = 1$, addition of fractures of length 1/2, (c) $i = 2$, addition of fractures of length 1/4, (d) $i = 3$, addition of fractures of length 1/8, (e) $i = 4$, addition of fractures of length 1/16 (f) $i = 5$, addition of fractures of length 1/32.

particular pattern. Note that this length is also the smallest fractal element in the pattern. However, if $\beta < b$ (as is usually the case), then $j > i$ and the limiting box size at which fractures can no longer be discerned will be larger than $r_{min} = 1/b^{imax+1}$ by an infinitesimally small amount. In this case, $j$max = INT[($i$max+1)log(b)/log(β)], where INT is a function that rounds a real number to the nearest integer.

[15] Equation (1), subject to the limiting values of r_{min} discussed above, can be used to evaluate the box counting fractal dimension of any synthetic fractal fracture pattern constructed with varying values of b, n and i, using any value of $1 < \beta \leq b$. For example, analytically box counting a fractal fracture pattern of $b = 2$, $n = 1$, and $i = 5$ (see Figure 1f) using $\beta = 1.1$, requires a minimum grid size of $r_{min} = 1/\beta^{jmax} = 1/1.1^{36}$ to confirm that the smallest fracture length present is $l_{min} = 1/b^{imax} = 1/2^5$. In addition to correctly identifying l_{min}, this analytical approach also yields a D_b value of 1.585 which is identical to the theoretical fractal dimension computed previously for this pattern.

2.3. Improved Numerical Box-Counting Algorithm

[16] The commercially available Benoit software (http://www.trusoft-international.com) is widely used for numerical box counting and enables the user to rotate the boxes and set β to a very small noninteger value >1 so that a large number of cell sizes can be generated. Thus it incorporates both the box rotate and box flex algorithms in finding the minimum number of occupied boxes for any given cell size.

[17] Within the Benoit platform, one can manually "turn off" points on the log-log plot so that the regression line is fitted to a subset of the data at the user's discretion. For our purpose, the side length of the largest box was fixed at $\frac{1}{2}$

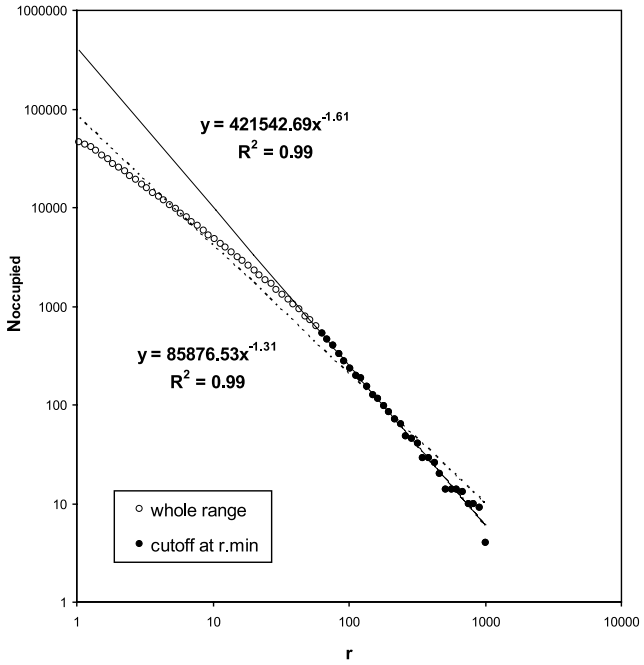

Figure 2. $N_{occupied}$ (number of occupied boxes) versus r (box size) for synthetic pattern with $b = 2$, $n = 1$, $i = 4$ including the whole range of data points ($s = 0.825$) and those for which $r < r_{min}$ were "turned off" ($s = 0.076$).

the width or length of the map, whichever was smaller. This ensured that $r < r_{max}$. The scaling factor of the box sizes was set at the smallest available value ($\beta = 1.1$), so that the number of box sizes (data points) was maximized in each case, thus generating a robust data set. The grid was rotated in 1° increments between 0 and 90° so that the algorithm determined the minimum $N_{occupied}$, required by *Hausdorff*'s [1919] boundary condition, from a large array of data points (90°/1° = 90) for each box size.

[18] The six synthetic patterns in section 2.1 were box counted in the Benoit platform and it was found that none of these fractal patterns yielded a straight line relationship when plotted on a log-log scale (e.g., Figure 2). This result is because no new elements are revealed and counted in the box counting algorithm when the box size r becomes smaller than the smallest fractal fracture element present. As a result, the $N_{occupied}$ versus r relationship deviates from its theoretical straight-line behavior on a log-log scale and becomes curvilinear. Therefore fitting a straight line to the entire range of data points returns a spurious fractal dimension and may further give the impression that the pattern under investigation is not a true fractal. A straight line, the slope of which gives the true fractal dimension of the pattern, should only be fitted to those data points for which r is larger than (or equal to) r_{min}. As discussed in section 2.2, when $\beta < b$ the limiting box size at which boxes appear unfilled is given by $r_{min} = 1/\beta^{jmax}$. Since both β and $j$max are known, those points for which $r < r_{min}$ are easily "turned off" in the plot (Figure 2), thereby yielding a better estimate of the true fractal dimension.

[19] Although r_{min} is known for the synthetic fractal fracture networks, it is unknown for natural patterns. Therefore a method for estimating a proxy value for r_{min} needs to be developed. Consider a linear regression equation fitted to $\log(N_{occupied})$ versus $\log(r)$ data by the method of least squares. The standard deviation of the slope, s, is estimated by [*Snedecor and Cochran*, 1989]

$$s = \sqrt{\frac{\sum_{k=1}^{n} (y_k - \hat{y}_k)^2}{(\nu - 2)\sum_{k=1}^{n} x_k^2}} \quad (3)$$

where y_k is observed $\log(N_{observed})$, $\hat{y}_k$ is predicted $\log(N_{observed})$, $x_k = \log(r)$, and ν is number of observations. For data points in the range $0 < r < r_{min}$, s decreases dramatically as $r \rightarrow r_{min}$. This relationship is because $y_k \rightarrow \hat{y}_k$ in the numerator of equation (3) as r values $< r_{min}$ are sequentially eliminated, while the increase in s due to the small reduction in ν (when $\nu \gg 2$) is minimal. In contrast, s gradually increases as $r \rightarrow r_{max}$ for data points in the range $r_{min} < r < r_{max}$. This relationship is because $(\nu - 2) \rightarrow 0$ in the denominator of equation (3) as $r \rightarrow r_{max}$, while there is minimal change in the overall goodness of fit determined by the numerator. These two competing relationships result in a minimum in the s versus r function at r_{min} that can be identified by the condition $ds/dr \rightarrow 0$.

[20] For each pattern, s from a linear regression equation fitted to the $\log(N_{occupied})$ versus $\log(r)$ plot, was noted in a systematic manner for points "turned off" at increasing r values. In some cases, because of statistical fluctuations in the data points, the ds/dr function sometimes jumped back to a small nonzero value after initially reaching a "local" zero. However, these local zeros never persisted beyond two consecutive r values. Therefore $ds/dr \rightarrow 0$ was identified by the ds/dr function remaining at zero for at least three consecutive r values (Figure 3). This condition defines the proxy r_{min} value denoted by r_{cutoff} (Figure 3). All box counting data points for which $r < r_{cutoff}$ were then excluded from fitting the regression line in the Benoit software.

3. Application to Synthetic Fractal Fracture Patterns

[21] The improved box counting algorithm described above was applied to the six synthetic fractal fracture patterns generated in section 2.1 (i.e., $b = 2$, $D = 1.585$, $i = 1$–6) to test how good an estimate it provides of the analytical parameters, r_{min} and D_b, when r_{cutoff} is used as the cutoff on the $\log(N_{occupied})$ versus $\log(r)$ plots. The resultant r_{cutoff} values were regressed against the known r_{min} values yielding the equation $y = 0.603x + 8.602$, with 5 degrees of freedom and a coefficient of determination, R^2, of 0.984. This analysis demonstrates a very strong positive association between the proxy, r_{cutoff}, and known r_{min} values that deviates from a strict 1:1 relationship. We shall show that this deviation had virtually no impact on the resulting estimates of D_b.

[22] The variation of D_b values estimated considering the whole range of data points, and following truncation based on the r_{min} and the r_{cutoff} values, with i, for the synthetic fractal fracture patterns described in section 2.1 is shown in Figure 4. From Figure 4, it can be seen that D_b computed using the whole range of r values increases systematically

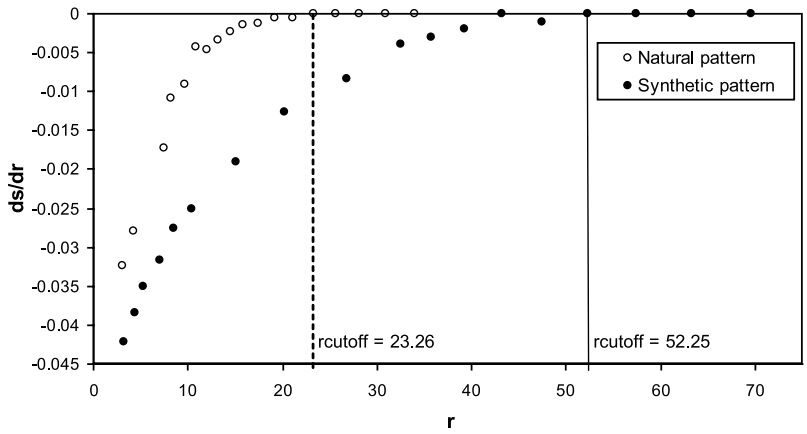

Figure 3. Determination of proxy r_{min} (r_{cutoff}) using ds/dr versus r for a synthetic pattern with $b = 2$, $n = 1$, $i = 4$ (theoretical $r_{min} = 63.23$) and a natural fracture pattern (map g from *Barton* [1995]). The location of r_{cutoff} is indicated by the vertical line for each case.

with increasing i, while consistently underestimating the theoretical D value. The associated error bars are relatively small and are consistent over the whole range of i. This result is because the same number of data points was used in the best fits regardless of the iteration level. On the other hand, the D_b obtained by not considering the r values smaller than r_{min} and r_{cutoff}, respectively, stabilize at $i = 3$ and approximate the theoretical D value of 1.585. The error bars around these D_b values become smaller with increasing i, which happens because the number of points used for calculating the slope of best fit increases with the iteration level, i.e., the error associated with the estimates increases as the r_{min} and r_{cutoff} values increase.

[23] The D_b values determined using the r_{min} and the r_{cutoff} truncation points were almost identical for $i \geq 3$ (Figure 4). However, both values resulted in a slight overestimate of the theoretical D value. While the reason for this bias is unclear, the magnitudes of the errors it produced were very small compared to those introduced by estimating D_b over the whole range of r (Figure 4). For $i > 3$ the modified box counting algorithm yielded estimates of D_b within ~2.2% of the known theoretical value.

[24] In general, these results indicate that using r_{cutoff} in place of r_{min} does not influence numerical box-counting estimates of the theoretical D value. Therefore r_{cutoff} may be used instead of r_{min} for evaluating the box-counting fractal dimension in the case of natural fractures, where a value for the latter is not normally available. Fracture lengths in natural networks commonly range over 1 or 2 orders of magnitude [*Barton*, 1995]. This size range is important because starting at $i = 4$, the lengths of our synthetic fractures were distributed over 2 orders of magnitude ($l_{max} = 1$ and $l_{min} = 1/b^i = 1/2^4 = 0.0625$). Thus the improved box-counting method should also work well in the case of natural fractures since they have the same relative length ranges as the synthetic patterns.

4. Application to Natural Fracture Networks

[25] *Walsh and Watterson* [1993] and *Gillespie et al.* [1993] have reported curvilinear box-counting plots for natural fracture networks similar to Figure 2 for our synthetic fractal fracture pattern. Furthermore, a close examination of the box-counting plots published by *Zhang and Sanderson* [1994] and *Barton* [1995] shows that they do not really fall on straight lines. The observed curvature raises questions about the fractal nature of these fracture patterns, and invites further investigation of natural networks using our modified box-counting algorithm. To facilitate this investigation, we selected 24 natural fracture patterns for analysis from *Odling* [1997] and *Barton* [1995].

4.1. Analysis of *Odling*'s [1997] Maps

[26] One detailed natural data set is a suite of 7 nested fracture patterns mapped in the same area of the Hornelen basin, Norway by *Odling* [1997]. Each map is a subset of the larger area [see *Bour et al.*, 2002, Figure 1] and is mapped from a lower elevation relative to the ground surface such that it represents a limited scale range of joint trace lengths controlled by the image resolution. The original 7 maps, received as encapsulated postscript files from Dr. Noelle Odling, were converted into bitmap images at 500dpi resolution using Adobe Illustrator. If the 720 m × 720 m pattern is self-similar, then all of the maps should have the same fractal dimension because one is essentially a scaled down version of the other.

[27] The r_{cutoff} and D_b parameters were evaluated for this data set using the modified box-counting algorithm. The former parameter, which is an estimate of the average minimum spacing between fractures in a natural pattern, changed systematically with the resolution (Table 1). It may

Table 1. Fractal Parameters for *Odling*'s [1997] Maps[a]

Map	Map Name	Area	Scale	r_{cutoff}, m	D_b	D_c
1	horn_ya	18 m × 18 m	1:102	0.35	1.80 ± 0.05	1.80 ± 0.10
2	horn_yb	55 m × 55 m	1:313	0.81	1.82 ± 0.04	1.77 ± 0.08
3	horn_yc	90 m × 90 m	1:511	1.33	1.82 ± 0.05	1.80 ± 0.05
4	horn_sa	90 m × 90 m	1:511	1.33	1.81 ± 0.05	1.80 ± 0.10
5	horn_sb	180 m × 180 m	1:1023	2.4	1.82 ± 0.04	1.82 ± 0.10
6	horn_sc	360 m × 360 m	1:2045	3.62	1.84 ± 0.04	1.85 ± 0.10
7	horn_sd	720 m × 720 m	1:4091	7.25	1.84 ± 0.04	1.88 ± 0.10

[a]Proxy r_{min} (r_{cutoff}), modified box-counting dimension (D_b), and capacity dimension (D_c) [*Bour et al.*, 2002].

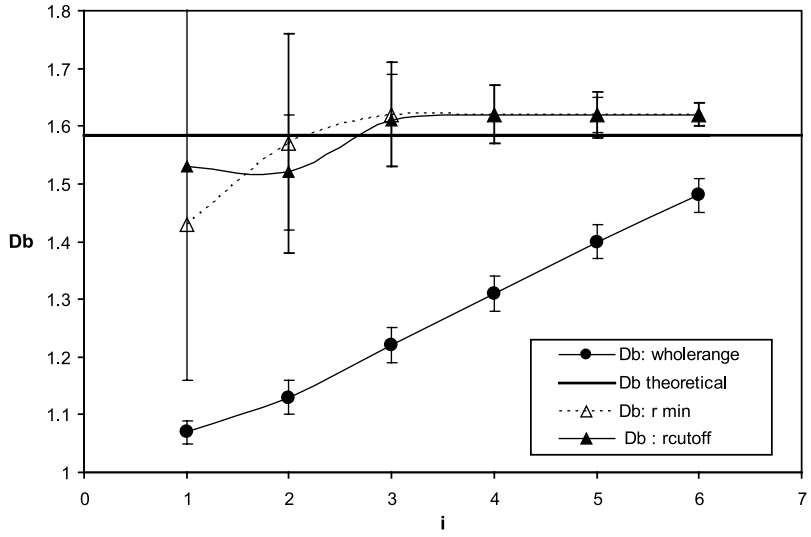

Figure 4. Variation of D_b with i for synthetic pattern $b = 2$, $n = 1$, D_b (±95% confidence intervals) computed using whole range of box sizes, box sizes larger than the r_{min}, and box sizes larger than r_{cutoff}.

be noted here that, given the fact that map 4 was photographed from a higher elevation than map 3, it is expected that the latter should yield a smaller r_{cutoff} value in meters. However, since a higher resolution camera was used in the case of map 4 as compared to map 3, this change compensated for the height effect (N. Odling, personal communication, 6 March 2006).

[28] Estimates of the box-counting fractal dimension, D_b, varied from 1.80 ± 0.05 at a scale of 1:102 to 1.84 ± 0.04 at a scale of 1:4091 (Table 1). Since there were no statistical differences between the different estimates of D_b at the 95% confidence level (i.e., $p < 0.05$) we can conclude that the fractal dimension of this network was constant throughout the different scales. Assuming that all maps come from the same fractal pattern, their combined box-counting results should plot as a single power law relation described by the equation $N_{map} = cr_m^{-D_b}$, where r_m is r expressed in terms of meters and c is a constant. The $N_{occupied}$ versus r data from all 7 maps were converted to meter scaling and plotted on a single log-log graph (Figure 5). The r_m values were computed using the expression $r_m = r_{pix} \times$ (side length of map area in m)/3473, where r_{pix} is r in terms of pixels, and 3473 is the length of the entire map in pixels. The $N_{occupied}$ values were accordingly adjusted using $N_{map} = N_{occupied} \times [720/(\text{side length of map area in m})]^{1.82}$, where 720 is the length of the largest map (in meters) and 1.82 is the fractal dimension for the pattern computed by averaging the D_b values in Table 1. The points from all the maps encompass a scale range of more than 3 orders of magnitude. Using this approach, Figure 5 shows in a very convincing manner that the Hornelen basin fracture pattern is a fractal over at least 3 orders of magnitude.

[29] *Odling*'s [1997] nested fracture maps were previously analyzed for their fractal characteristics by *Bour et al.* [2002]. Bour et al. computed the capacity dimension, D_c (equivalent to D_b, but estimated using an alternative

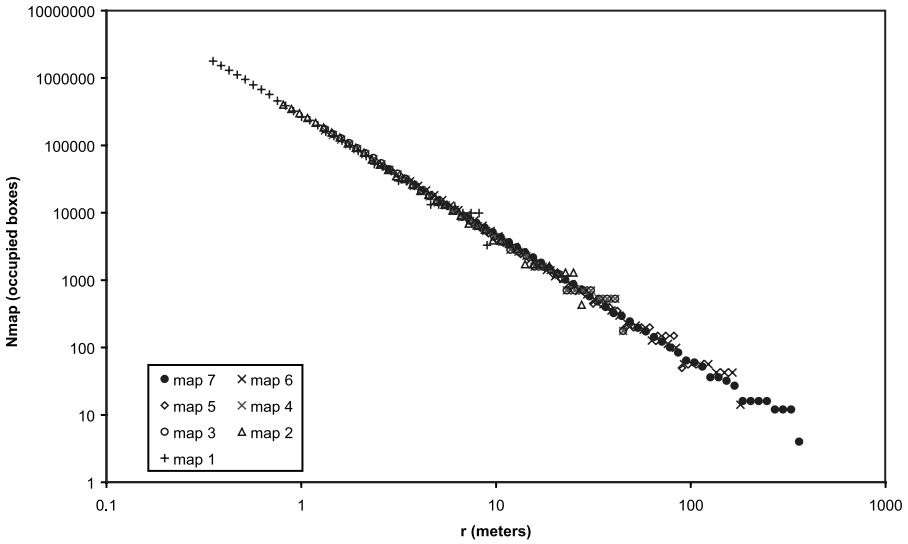

Figure 5. N_{map} versus r_m for maps 1–7 from *Odling* [1997].

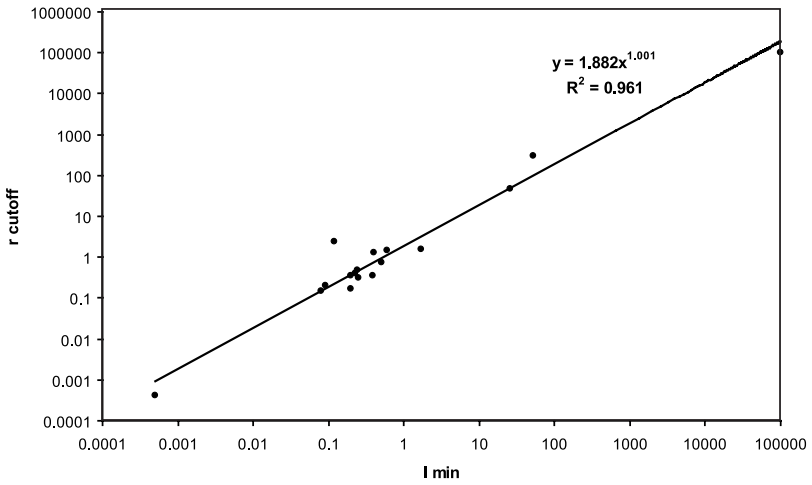

Figure 6. Relationship between l_{min} and r_{cutoff} for *Barton*'s [1995] maps.

technique) at each scale. Comparing our estimates of D_b with those for D_c from *Bour et al.* [2002] in Table 1, it can be seen that D_b lies within a narrower range and exhibits less variation than D_c in terms of the 95% confidence limits. This increase in precision and accuracy suggests that our improved box-counting method is better able to identify the existence of an underlying fractal pattern over multiple scales than capacity dimension analyses.

4.2. Analysis of *Barton*'s [1995] Maps

[30] Using the modified box-counting approach, we reanalyzed a series of 17 previously published fracture trace maps from a variety of tectonic settings, lithologies and scales [*Barton*, 1995]. All maps were scanned at 500 dpi in B/W line mode using a standard scanner into Photoshop. They were subsequently rotated and cropped in the shape of a rectangle so as to exclude any blank "unmapped" areas while including all of the mapped fractures. Box-counting analyses of different digitized versions of these maps have been reported previously by *Barton* [1995] and *Berkowitz and Hadad* [1997]. In this section, we present our results and compare them with those of *Barton* [1995] and *Berkowitz and Hadad* [1997].

[31] A plot of the estimated r_{cutoff} values for these maps versus the smallest fracture lengths (l_{min}) reported by Barton shows two important characteristics (Figure 6). First, it displays the scale range of the maps: from microscopic (map q) to that of transform faults (map p) covering over 8 orders of length magnitude. Second, it shows that r_{cutoff} was positively correlated with the l_{min} parameter (R^2 = 0.961), such that the former can be a very good estimate of the latter. Since the regression equation reported in Figure 6 is based on multiple data sets, has a very high R^2 value, and covers such a wide range of scales, it can be used with confidence for interpolation purposes. It can also be easily rearranged and used by researchers to estimate r_{cutoff}, thus eliminating the need to perform multiple fits for the $ds/dr \rightarrow 0$ analysis (see Figure 3) in the case of fracture networks for which l_{min} is known or has been measured independently.

[32] The D_b values estimated using our modified box-counting method ranged from 1.56 ± 0.02 to 1.79 ± 0.02 (Table 2). Comparing these values with those of *Barton*'s [1995] and *Berkowitz and Hadad*'s [1997], one can see that

Table 2. Fractal Parameters for *Barton*'s [1995] Maps[a]

Map	Location	l_{min}, m	r_{cutoff}, m	D_b	D_b Whole	D_b Barton	D_b B&H
a	Yucca Mountain, Nevada	0.25	0.32	1.64 ± 0.01	1.55	1.52	1.85 ± 0.02
b	Yucca Mountain, Nevada	0.5	0.74	1.56 ± 0.02	1.45	1.38	1.74 ± 0.03
c	Yucca Mountain, Nevada	0.39	0.36	1.62 ± 0.02	1.54	1.50	1.87 ± 0.02
d	Yucca Mountain, Nevada	0.59	1.43	1.71 ± 0.01	1.61	1.61	1.71 ± 0.03
e	Yucca Mountain, Nevada	0.23	0.4	1.74 ± 0.02	1.56	1.59	1.91 ± 0.02
f	Yucca Mountain, Nevada	0.24	0.47	1.64 ± 0.03	1.54	1.54	1.87 ± 0.02
g	Yucca Mountain, Nevada	0.2	0.17	1.77 ± 0.02	1.65	1.70	1.98 ± 0.00
h	Cedar City, Utah	1.7	1.56	1.62 ± 0.02	1.55	1.50	1.90 ± 0.02
i	Lannon, Wisconsin	0.09	0.2	1.75 ± 0.04	1.63	1.60	1.91 ± 0.02
j	Morrison, Colorado	0.12	2.35	1.79 ± 0.02	1.67	1.50	1.89 ± 0.03
k	Valley of Fire, Nevada	0.2	0.36	1.78 ± 0.02	1.68	1.58	1.88 ± 0.02
l	Mexican Hat, Utah	0.08	0.15	1.66 ± 0.02	1.58	1.52	1.93 ± 0.02
m	Yucca Mountain, Nevada	53	306.92	1.75 ± 0.06	1.49	1.49	1.95 ± 0.01
n	Juneau, Alaska	0.4	1.28	1.69 ± 0.02	1.50	1.48	1.82 ± 0.02
o	Goldhill, Colorado	26	46.16	1.70 ± 0.02	1.61	1.52	1.92 ± 0.01
p	South Atlantic seafloor	99000	103000	1.63 ± 0.02	1.47	1.32	1.77 ± 0.04
q	Timmins, Ontario	0.0005	0.000412	1.69 ± 0.03	1.47	1.58	1.88 ± 0.01

[a]Reported l_{min}, proxy r_{min} (r_{cutoff}) and box counting fractal dimensions evaluated using the modified box-counting technique (D_b), using the whole data range of data points (D_b whole), by *Barton* [1995] (D_b Barton), and *Berkowitz and Hadad* [1997] (D_b B&H).

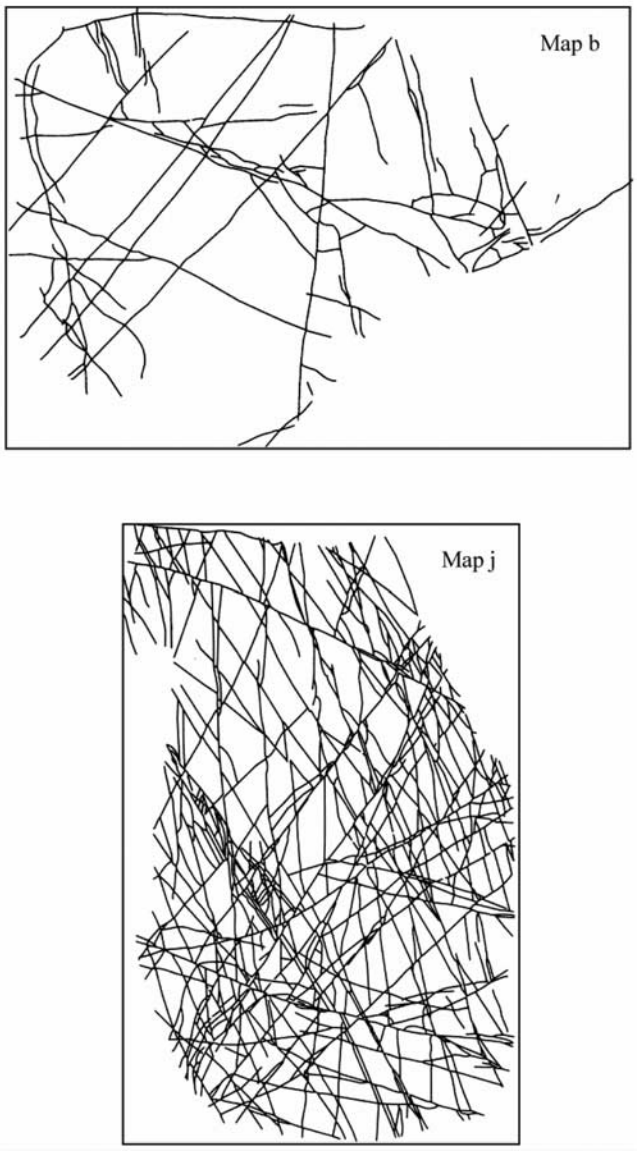

Figure 7. *Barton*'s [1995] maps (top) b and (bottom) j with lowest and highest D_b values respectively, showing differences in fracture complexity (adapted from *Barton and La Pointe* [1995] with kind permission of Springer Science and Business Media).

the former are underestimates while the latter are overestimates (Table 2). Table 2 shows that our box-counting results obtained by not "turning off" the data points for which $r < r_{cutoff}$ (i.e., considering the whole range of data points) returned consistently lower estimates of D_b, the magnitudes of which are very similar to those reported by *Barton* [1995]. In fact, for maps d, f, and m the values are exactly the same. This clearly demonstrates that if the data points for which $r < r_{cutoff}$ are considered for fitting the straight line in a box-counting analysis, we end up with less accurate D_b values, even though the R^2 values may be high.

[33] The question still remains as to the differences between our results and those of *Berkowitz and Hadad* [1997]. Berkowitz and Hadad suggest that cropping (with some loss of data) was responsible for their high D_b values. However, similar cropping did not have any significant effect on D_b in the case of our modified box-counting algorithm [*Roy*, 2006]. Instead, we suggest that the discrepancy may be related to differences in the map resolution and/or the scaling factor, β, employed in the two studies. For instance, one of their digitized maps (map b) was only 128×128 pixels, whereas ours was 2063×1463. The lower resolution employed by Berkowitz and Hadad may have yielded inaccurate box counts for the smallest box sizes. Furthermore, the larger the β value, the fewer the number of points on the box-counting curve. Their plot for map b has only 5 data points whereas in our modified box-counting plot there were 28. This difference is because the scaling factor of the box sizes was $\beta = 2$ in their analyses as opposed to $\beta = 1.1$ in ours. The importance of a robust data set cannot be overemphasized since the use of a just a few points to fit a straight line has already met with criticism and raised doubts about the fractal nature of the fracture network under investigation [e.g., *Bonnet et al.*, 2001].

[34] The D_b estimates from the modified algorithm show in general that, the greater the complexity of the network, the greater is the box-counting dimension (Figure 7). This observation may in turn be related to physical properties of the fractured media. For example, recent studies based on percolation theory suggest that the magnitude of the D_b value controls the extent of fracture connectivity in a network [*Bour and Davy*, 1997, 1998; *Berkowitz et al.*, 2000]. Higher D_b values imply a greater degree of fracture connectivity and thus increased propensity for fracture flow and the transport of miscible or immiscible chemicals [*Acuna and Yortsos*, 1995; *Doughty and Karasaki*, 2002]. In this context, small differences in the magnitude of D_b can have a large impact on fracture connectivity and flow processes, so it is important that this parameter be estimated as accurately as possible.

5. Conclusions

[35] Analytical and numerical box-counting analyses of synthetic fractal fracture patterns facilitated the development of a proxy r_{min} parameter known as r_{cutoff}. If points on the $\log(N_{occupied})$ versus $\log(r)$ plot for which $r < r_{min}$ or r_{cutoff} are "turned off," then the remaining points can be fitted by a straight line whose negative slope estimates the fractal dimension of the pattern. The results from these analyses demonstrate that our modified box-counting technique is accurate and precise, and can be used with any fracture network to check for fractal scaling, and if appropriate to evaluate the smallest fracture spacing and fractal dimension.

[36] Our analyses of *Odling*'s [1997] maps from the Hornelen basin in Norway demonstrate that natural fracture patterns can indeed be fractals and repeat themselves over at least 3 orders of magnitude. Our analyses of *Barton*'s [1995] maps indicate that the r_{cutoff} parameter is also an excellent predictor of the reported minimum fracture length. Our estimated D_b values were very different from the values reported both by *Barton* [1995] and *Berkowitz and Hadad* [1997] for the same data sets. For each of the 17 maps analyzed, our "improved" D_b value was consistently greater than that of *Barton*'s [1995] and less than that of *Berkowitz and Hadad*'s [1997]. The modification in the

box-counting algorithm employed by us is the reason for the difference between our results and those of *Barton*'s [1995]. On the other hand, differences in map resolution and the box size scaling factor appeared to be the main reasons for our values being different from those of *Berkowitz and Hadad* [1997].

[37] Although many workers have argued over the fractal nature of fractures, some networks can be truly self-similar such that their geometries are described by a single fractal dimension. The magnitude of D_b controls the percolation and connectivity properties of fractured media. However, it should be noted that fracture networks with the same fractal dimension often look very different from each other. Therefore future research is suggested on the application of additional quantitative parameters, such as lacunarity [*Turcotte*, 1997], to the characterization of natural fracture patterns.

[38] **Acknowledgments.** We would like to thank Noelle Odling for kindly providing us with the original encapsulated postscript files of the Hornelen fracture maps which have been used in our analysis in section 4.1.

References

Acuna, J. A., and Y. C. Yortsos (1995), Application of fractal geometry to the study of networks of fractures and their pressure transient, *Water Resour. Res.*, *31*, 527–540.

Barton, C. C. (1995), Fractal analysis of scaling and spatial clustering of fractures, in *Fractals in the Earth Sciences*, edited by C. C. Barton and P. La Pointe, pp. 141–178, Plenum, New York.

Barton, C. C., and P. La Pointe (Eds.) (1995), *Fractals in the Earth Sciences*, Plenum, New York.

Berkowitz, B., and A. Hadad (1997), Fractal and multifractal measures of natural and synthetic fracture networks, *J. Geophys. Res.*, *102*, 12,205–12,218.

Berkowitz, B., O. Bour, P. Davy, and N. Odling (2000), Scaling of fracture connectivity in geological formations, *Geophys. Res. Lett.*, *27*, 2061–2064.

Bonnet, E., O. Bour, N. E. Odling, P. Davy, I. Main, P. Cowie, and B. Berkowitz (2001), Scaling of fracture systems in geological media, *Rev. Geophys.*, *39*, 347–383.

Bour, O., and P. Davy (1997), Connectivity of random fault networks following a power law fault length distribution, *Water Resour. Res.*, *33*, 1567–1583.

Bour, O., and P. Davy (1998), On the connectivity of three-dimensional fault networks, *Water Resour. Res.*, *34*, 2611–2622.

Bour, O., P. Davy, C. Darcel, and N. Odling (2002), A statistical scaling model for fracture network geometry, with validation on a multiscale mapping of a joint network (Hornelen Basin, Norway), *J. Geophys. Res.*, *107*(B6), 2113, doi:10.1029/2001JB000176.

Doughty, C., and K. Karasaki (2002), Flow and transport in hierarchically fractured rock, *J. Hydrol.*, *263*, 1–22, doi:10.1016/S0022-1694(02)00032-X.

Gillespie, P. A., C. B. Howard, J. J. Walsh, and J. Watterson (1993), Measurement and characterization of spatial distributions of fractures, *Tectonophysics*, *226*, 113–141.

Hausdorff, F. (1919), Dimension und ausseres Mass, *Math. Ann.*, *79*, 157.

La Pointe, L. R. (1988), A method to characterize fracture density and connectivity through fractal geometry, Int, *J. Rock Mech. Min. Sci. Geomech. Abstr.*, *25*, 421–429.

Mandelbrot, B. B. (1983), *The Fractal Geometry of Nature*, 468 pp., W. H. Freeman, New York.

Odling, N. E. (1997), Scaling and connectivity of joint systems in sandstones from western Norway, *J. Struct. Geol.*, *19*, 1257–1271.

Pruess, S. A. (1995), Some remarks on the numerical estimation of fractal dimension, in *Fractals in the Earth Sciences*, C. C. Barton and P. La Pointe, pp. 65–75, Plenum, New York.

Roy, A. (2006), A quantitative study of scaling properties of fracture networks, M. S. thesis, 103 pp., Univ. of Tenn., Knoxville.

Sammis, G. C., R. H. Osborne, J. L. Anderson, M. Banerdt, and P. White (1986), Self-similar cataclasis in the formation of fault gouge, *Pure Appl. Geophys.*, *124*, 53–78.

Samuel, J. (1988), A method for estimating the Hausdorff dimension of a planar line pattern, M. S. thesis, Colo. Sch. of Mines, Golden.

Snedecor, G. W., and W. G. Cochran (1989), *Statistical Methods*, 8th ed., 503 pp., Iowa State Univ. Press, Ames.

Turcotte, D. L. (1997), *Fractals and Chaos in Geology and Geophysics*, 398 pp., Cambridge Univ. Press, New York.

Walsh, J. J., and J. Watterson (1993), Fractal analysis of fractal patterns using the standard box-counting technique: Valid and invalid methodologies, *J. Struct. Geol.*, *15*, 1509–1512.

Zhang, X., and D. J. Sanderson (1994), Fractal structure and deformation of fractured rock masses, in *Fractals and Dynamic Systems in Geoscience*, edited by J. H. Kruhl, pp. 37–52, Springer, Frankfurt, Germany.

W. M. Dunne, L. D. McKay, E. Perfect, and A. Roy, Department of Earth and Planetary Sciences, University of Tennessee, 1412 Circle Drive, Knoxville, TN 37996-1410, USA. (eperfect@utk.edu)